Carpathian Journal of Earth and Environmental Sciences, August 2019, Vol. 14, No. 2, p. 449 - 462; DOI:10.26471/cjees/2019/014/094

THE LA-ICP-MS U-Pb AGES AND Lu-Hf ISOTOPE OF DETRITAL ZIRCONS FROM THE BAYANKALAANKALA GROUP IN DARI AREA: IMPLICATION FOR THE PROVENANCE

Jiawei CUI[1]* & Junyi SUN[2]

[1] Institute of Geomechanics, Chinese Academy of Geological Sciences, Beijing, China
**Corresponding author. E-mail address: 1cuijiawei1@163.com*
[2]State Key Laboratory of Geological Processes and Mineral Resources, China University of Geosciences (Beijing), Beijing 100083, China

Abstract: Songpan-Ganzi Orogenic belt is covered by thick Triassic turbidite complex-Bayankala Group. The provenance of Triassic turbidites is still controversial. In order to constrain the provenance of the siliciclastic rocks, we carried out La-ICP-MS zircon U–Pb dating and Hf isotope analyses on 158 detrital zircons obtained from Bayankala group. Analysis on the LA-ICP-MS U-Pb ages of the detrital zircon from Bayankala Mountain Group indicates that the yougest age is 218Ma and it was intruded by the granite (209 M a). Therefore, we suggest that the formation age is 209-218Ma. The detrital zircons from Bayankala group exhibit wide age spectra with three dominant populations of 212-500Ma, 1711-2000Ma, and 2200-2500Ma. The εHf(t) range from-11.69- +16.41 and TDM2 age exhibit a wide age spectrum. Generally, three major peaks exist at 3.5–4.5 Ga, 750–1250 Ma, and 290–450 Ma. Combined the geological background, we suggest that the Bayankala Group was mainly derived from Qinling, Qilian, and Kunlun orogens along the southern margin of the North China Craton with minor the South China. In addition, our Lu–Hf isotopic results also reveal that the Phanerozoic magmatic rocks in central China had been the primary products of crustal reworking with insignificant formation of a juvenile crust.

Key words: Zircon U-Pb age, Lu–Hf isotopes; The Bayankala Group; The north of Songpan-Ganzi fold belt

1. INTRODUCTION

Songpan-Ganzi orogenic belt is located in the northeastern Tibetan Plateau. It is covered by the Triassic turbidities complex (Brugier et al., 1997; Ding et al., 2013; Enkelmann et al., 2007; Gu, 1994; Pullen et al.,2008; Nie et al., 1994; Zhang et al., 2008), which may record crustal material that has been denuded or is no longer exposed.

Over the last decade, many researches have been focused on the tectonic setting of Songpan-Ganzi Orogenic Belt and the provenance of the Triassic turbidites (Nie et al. 1994; Gu et al., 2002; Zhou & Graham 1996; Brugier et al., 1997; Weislogel et al., 2006, 2010; She et al., 2006; Liu et al., 2008; Zhang et al., 2008, 2012, 2014; Enkelmann et al., 2007; Weislogel 2008; Ding et al., 2013). Because of the strong deformed metamorphism, the provenance of Triassic turbidites is still controversial: ultrahigh-pressure metamorphosed belt of Dabieshan (Nie et al., 1994), Qinling-Dabie Orogenic Belt (Zhou & Graham, 1996; Weislogel et al., 2006, 2010; Enkelmann et al., 2007), Kunlun Mountain Plate (She et al., 2006; Zhang et al., 2012), the South China block (Brugier et al., 1997), and Qiangtang Plate (Zhang et al., 2008; Zhang et al., 2012). It is a common view that Triassic turbidites sedimentary rock is not of a single origin, but of a mixed sediment provenance (Ding, et al, 2013; Chen et al., 2003). The formation age of the Bayankala group is still controversial: Huang and Chen (1987) suggested that the formation age of Bayankala Group was 230-203Ma. Enkelmann et al., (2007) suggested that the formation age is 205Ma based on Ar-Ar dating. Ding et al., (2013) suggest that the formation age is 155Ma, according to the youngest detrital zircon age which is 157Ma and is same with the age of remnant ocean of the Paleo-Tethys Ocean.

Zircon is an extremely stable mineral that can survive erosion or metamorphism and can provide valuable information for evolution of the continental

crust (Taylor & McLennan 1995; Li et al., 2002). U–Pb and Lu–Hf isotope of detrital zircons can provide important constraints for evaluating potential source regions, which have been widely applied to reveal the evolution of crust (Wilde et al. 2001; Griffin et al. 2004; Veevers et al. 2005; Hawkesworth and Kemp. 2006; Yang et al. 2006). Here we report 158 U–Pb age and 88 Hf isotopic compositions of detrital zircons from Triassic sandstone-Bayankala Group from the Songpan terrane of the Songpan–Ganzi turbidite complex (Fig. 1), in an attempt to constrain the sources of Bayankala Group.

2. GEOLOGICAL SETTING

The Songpan–Ganzi orogenic belt is bound in the southwest with the Qiangtang block and the Jiangda arc by the Jinsa suture, in the northwest with the Qaidam block by the Kunlun suture, in the northeast with the North China Craton by the Qilian–Qinling sutures, and in the east with the South China block by the Longmen fault zone (Zhang 2001, Zhang et al., 2014; Fig. 1a). This terrane had been believed to be floored by an oceanic crust (Nie et al. 1994; Zhou and Graham 1996). Although it is generally believed to be floored by an oceanic crust, seismic profiling indicates that the Songpan–Ganzi complex is underlain by ~30 km of felsic-intermediate continental crust (Zhang 2001; Wang et al. 2011). Because lack of fossils and intense deformation has hindered the information of the geologic evolution of the Songpan-Ganzi complex (GBGMR, 1989; Weislogel et al., 2010).

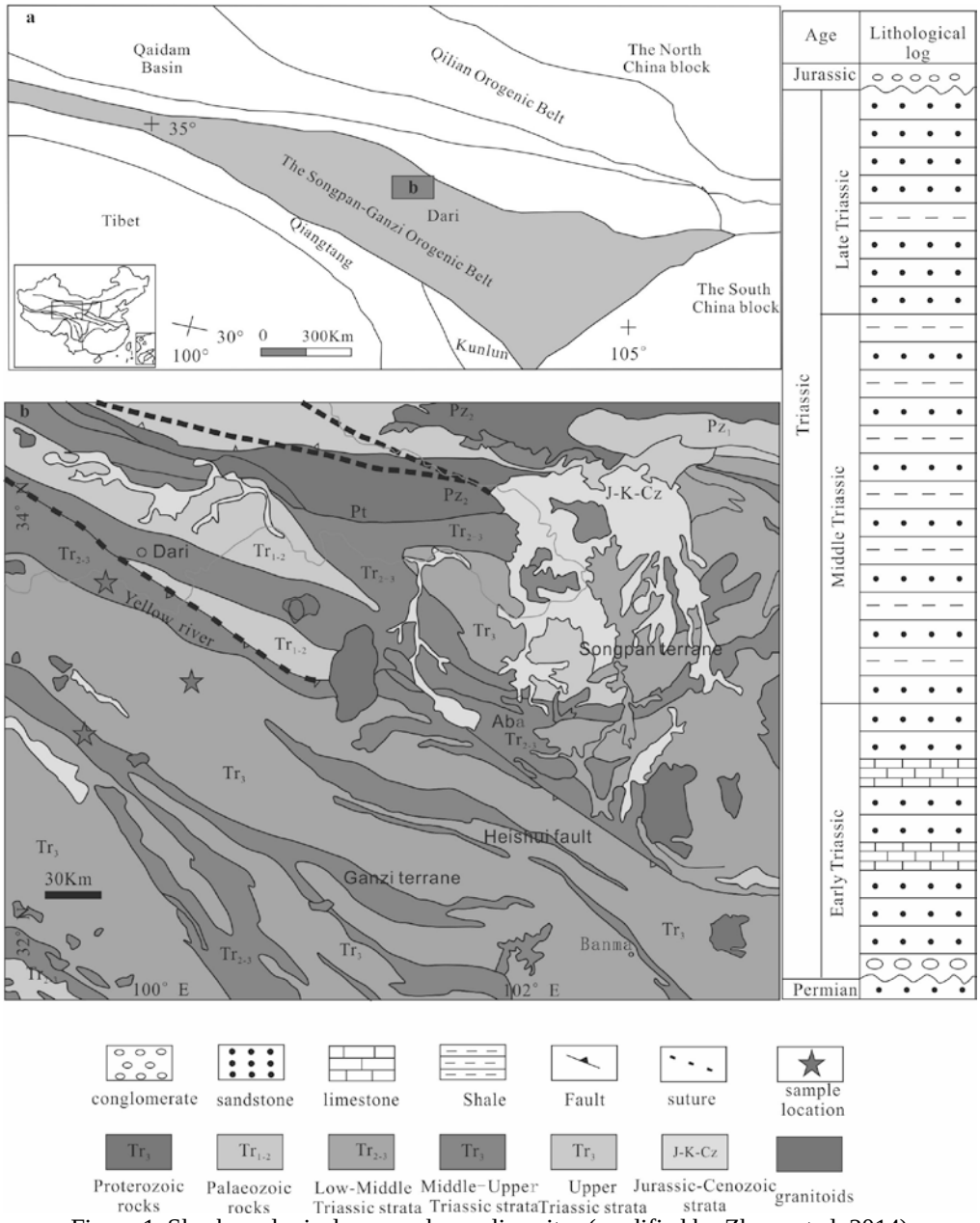

Figure 1. Skech geological map and sampling sites (modified by Zhang et al.,2014)

It was covered by Triassic turbidites-Bayankala group which contains an up to 10 km-thick succession that was accumulated during the late Middle Triassic to the Late Triassic (Cohen et al. 2013). It is conformably underlain by thin pre-Triassic chert, shale, and siltstone (Nie et al. 1994; Zhou and Graham 1996) and was intruded by Triassic granite (Cui et al.,2016). The Bayankala group can be divided into three parts.(Cui et al.,2016).The lower part of the the Bayankala group is consists of siliceous rocks with minor small gravels. The middle of the Bayankala group is consist of interbedded sand and mud. The upper part of the Bayankala group is consist of sand (GBGMR, 1989.

3. ANALYTICAL METHODS

3.1 Zircon U–Pb dating

Three samples were used for zircon U–Pb analysis. Prior to analysis, zircons were separated using standard heavy liquid techniques before individual zircons were hand-picked under an optical microscope to remove grains with visible impurities. The resulting zircon separates were mounted in epoxy resin before being imaged using reflected light and cathodoluminescence (CL) to identify internal structures and to select points for analysis. These zircons were analyzed by LA–ICP–MS at the State Key Laboratory of Geological Processes and Mineral Resources, Wuhan, China, using the approached outlined by Liu et al. (2010). The resulting data were standardized using a 91500 standard zircon and a NIST610 glass standard, and were reduced using Isoplot v. 3.0 (Ludwig, 2003), yielding weighted mean ages with 2σ uncertainties.

3.2 Lu-Hf isotopic

Zircon Hf isotopic compositions were determined by LA–MC–ICP–MS and a Neptune Plus instrument combined with a Geolas 2005 excimer ArF laser ablation system at the State Key Laboratory of Geological Processes and Mineral Resources, Wuhan, China.

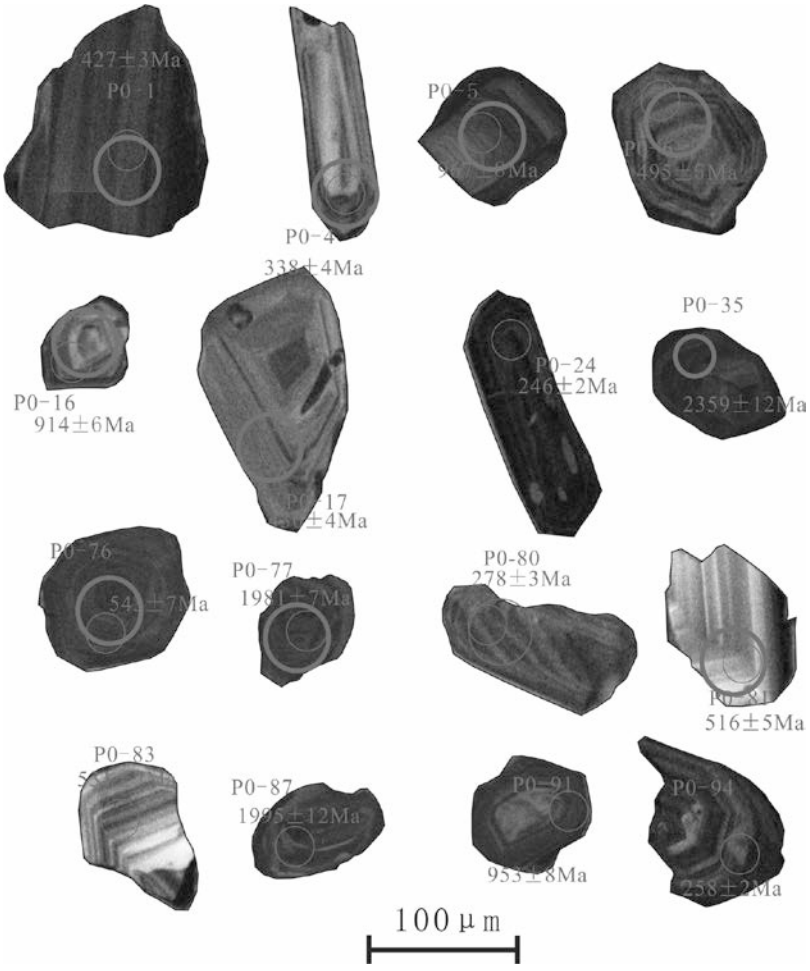

Figure 2. CL photographs of zircons from the CTR with test point location and ages marked. The solid line circles indicate the positions for U-Pb analysis and the dotted circles indicate the positions for Hf isotope analyses.

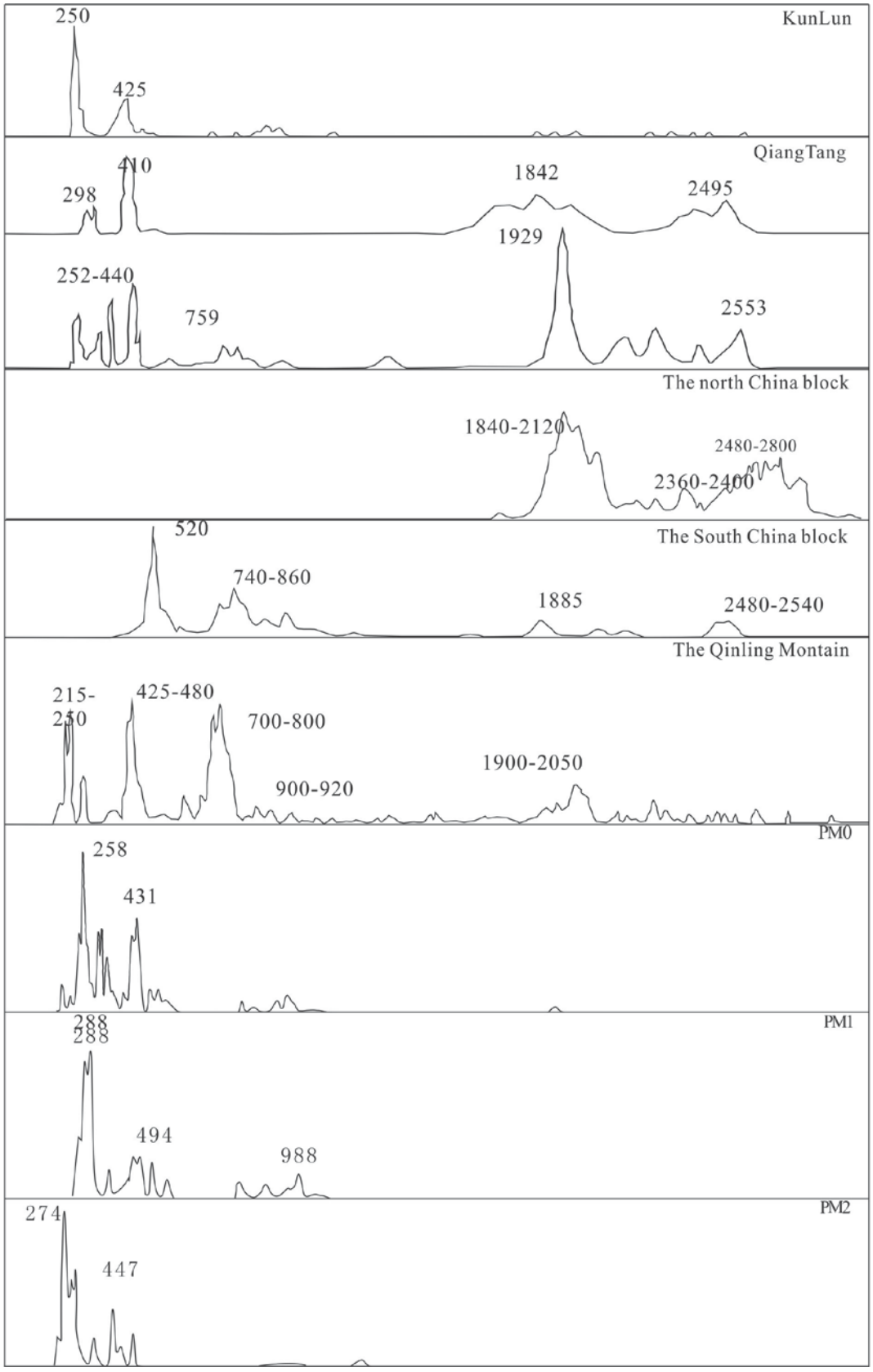

Figure 3. Distribution curves for Ages of U-Pb of clastic zircons

These analyses used a 44 μm spot size, an 8 Hz repetition rate, and a laser power of 60 mJ/pulse. Operating conditions were the same as those described by Hu et al. (2014) and the resulting data was reduced using ICPMSDataCal (Liu et al., 2010).

4. ANALYTICAL RESULTS

4.1 Zircon analysis

Representative three samples of the lower of Bayankala group (PM0), the middle of Bayankala group (PM1) and the upper of Bayankala group (PM2) were used for zircon LA-ICP-MSU–Pb dating. The zircon characteristics of the three samples are described in Figure 2.

The zircons from three samples exhibit smililar characteristics and can be divided into two groups approximately based on their CL images (Fig. 2). The zircons whose ages is above 1000Ma show rounded sharp and small size, with length of the long axis ranging from 60μm-100μm, and the ratio of long axis to short axis ranges between 1:1 and 1.5:1. Zircons whose ages are relatively younger mostly show sub-rounded or rounded, and their grains are relatively large, with long axis length ranging between 120μm-150μm, and the ratio of long axis to short axis ranging from 3:1 to 2:1. Most zircons are oscillatorily zoned and minor are homogeneous in CL images and all zircons have obviously changing Th/U ratios, ranging from 0.17 to 1.2. The sample zircons are characterized by three dominant populations of 218-288 Ma, 418-456 Ma and 881-970 Ma (Fig. 3 and Table 1).with small amount distributing around 1800Ma (Table 1 and Fig. 3), and almost all the points of data fall on the harmony curve. (Belousova et al., 2002).

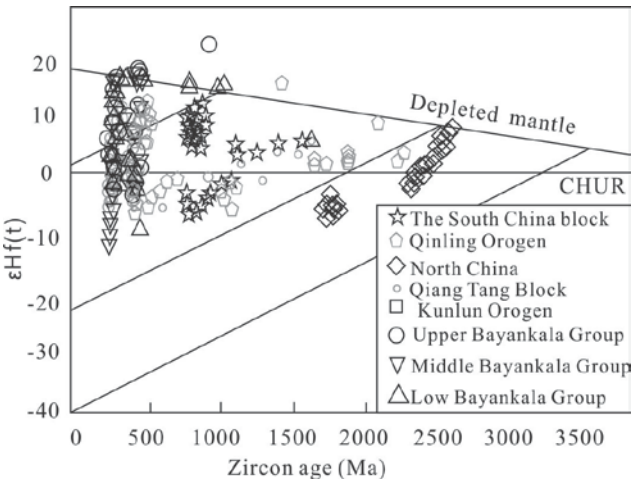

Figure 4. U–Pb age versus εHf(t) value plots of concordant detrital zircons from the Triassic flysch in the Songpan–Ganzi complex, North China – Yang et al. 2006, 2009) and references; Qiangtang – Tan et al. (2009); Qilian – Song et al. (2010); Qinling – Wang et al. (2009) and references therein; The South China block – Li et al. (2002); Liu et al. (2008); Yu et al. (2008) and references therein.

4.2 Hf isotopic characteristics of zircons obtained from the Bayabkala group

Eighty-eight zircons from the samples were analysed for Hf-isotope composition (Table 2). Zircons from all three samples exhibit large ranges in εHf(t) values. All of the zircons from the three samples lie above the chondrite and below the depleted mantle Hf-isotope evolution reference line (Fig. 4). The initial $^{176}Lu/^{177}Hf$ range from 0.000241 to 0.002218, corresponding with εHf(t) of -11.69-+16.41, most zircons within single age populations have positive εHf(t) values, and others have negative εHf(t) values (Fig. 4) while the Precambrian zircons are dominated by negative εHf(t) values, while nearly one half of the Palaeozoic and Mesozoic zircons have positive εHf(t) values. These Hf continental model ages (TDM2) age exhibit a wide age spectrum. Generally, three major peaks exist at 3.5–4.5 Ga, 750–1250 Ma, and 290–450 Ma (Fig. 3).

5. DISCUSSION

5.1 Formation age of Bayankala Mountain Group

Lack of high-precision chronology data and fossils, especially those invertebrates fossils that can be used for determining the age, and therefore, the formation age of Bayankala Group is still controversial. The youngest detrial zircon age is 218 Ma and the age of the granite which intruded into Bayankala Group is 209Ma (Cui et al., 2016). Therefore, We suggest that the formation age is 209-218Ma.

5.2 Sediment provenance analysis for Bayankala Group

Age spectra of all Bayankala group show a prominent U–Pb age peak at 529–247 Ma and typically give both positive and negative εHf(t) values, which is similar to the age distribution of Kunlun Plate (Cowgill et al., 2003; Schwab et al., 2004; Chen et al., 2003; Weislogel et al., 2006; 2010； Ding et al, 2013), Qiling belt and Qiangtang Plate (Zhang et al., 2015; Ding et al., 2013). The paleocurrent direction is north, north-west-south-east (Zhou & Graham, 1996; Weislogel, 2008, Weislogel et al., 2010; Ding et al., 2013), which also indicates that the sedimentary rocks of Triassic Period originate from Kunlun Plate, Qinling belt and Qiangtang plate.

The Qinling orogen can be divided into north Qinling orogen and south Qinling orogen. The north Qinling belt contains Andeantype margin accretionary-arc complex (400–300 Ma) (Zhang et al.,1994), the collision-type granites with ages of 323–

262 Ma (Zhang et al. 1994) and primary early Palaeozoic (501–410 Ma) metamorphic events (Wang et al. 2009), but only the arc could have constituted a significant source for the 400–300 Ma zircons of our samples. The south Qinling contains the Middle Devonian–Upper Triassic collision-related crystalline rocks that records peak igneous activity at 345–300 Ma (Nie et al. 1994; Zhang et al., 2012), but it could not have supplied zircons in our samples because the Yangtze craton possibly did not serve as a significant source area for our samples as discussed above. Therofore, we can conclude that the Qinling, Qilian, and Kunlun orogenic could have been the significant sources.

The zircon age distribution obtained from Bayankala group is different from that from Qiangtang Block (Zhang et al., 2015; Ding et al., 2013) (Fig. 3). The Lu-Hf isotope data also suggest that our samples are much different from those from the Qiangtang Block (Zhang et al., 2015). As a result, we suggest that Qiangtang Block is not the source of the Bayankala Mountain Group.

Another prominent U–Pb age peak at 881-970 Ma could derive from the South China Craton (Fig. 3 and Table 1) are marked by both positive and negative εHf(t) values (Li et al., 2002; Liu et al., 2008; Yu et al., 2008). This signature is generally used to distinguish detrital sources of the Yangtze Craton from those of the North China Craton (Li et al. 2002; Zhang et al., 2014; 2015).

The Palaeoproterozoic–Archaean zircon age populations well fall into the overlap of Hf isotope between the North China and the south China craton. The South China block showed respectively two peak periods, i.e. 2900Ma-2950Ma and 2000Ma-2100Ma, while the zircons from Bayankala Group in this paper present almost no age data between 2900-2950M, and very few data ranging from 2000-2100Ma. At Middle Neoproterozoic, The South China block formed into a stable basement, and experienced two tectonic thermal events, Sipu Orogeny movement (1100~1000 Ma) and Jinning-Chengjiang Movement (800~700Ma) (Li et al., 2002; Li et al., 2003; Chen et al., 2003). According to the geophysical data, the deep Songpan–Ganzi complex was obducted over beneath the Yangtze Craton (Zhang 2001). Together with the W- to NW-oriented palaeocurrent indicators (Zhang et al., 2015), we can deduced that the South China block may serve as a minor source area.

The sample show consistent component of North China block affinity 1.8–1.9 and 2.4–2.5 Ga zircon grains along with Paleozoic zircon populations (215– 280 Ma) and south- to southwest-directed paleocurrent indicators. The Hf isotope of our sample is consistent with the data obtained from the zircons from North China Plate whose ages are over 1.9 Ga are of positive values (Ding et al, 2013). Therefore, We suggest that North China is one of the major source of clastic rocks of the Bayankala Group . (Zhang et al, 2014; Ding et al., 2013).

Therefore, the Bayankala group sandstones yield age probability density functions consistent with the Qinling, Qilian, and Kunlun orogens along the southern margin of the North China Craton (Fig. 3). Meanwhile, the South China may also serve as minor source areas.

5.3 Crustal growth of the Songpan terrane

None of the magmatic zircons from our three new Triassic sandstone samples have εHf(t) values identical to depleted mantle values. This indicates that the studied zircons contain variable amounts of recycled crustal materials. For such zircons, the two-stage Hf model age (TDM2) calculated by using the upper crustal Lu/Hf value (0.0093) is a better approximation of crustal formation ages (Hawkesworth & Kemp 2006; Liu et al. 2008). Our three samples are characterized by a common prominent group of Hf crust formation model ages at 4.1–0.3 Ga,. However, few zircons from the Upper–Middle Triassic show the Phanerozoic model ages, indicating that the Phanerozoic igneous rocks in central China were mostly products of crustal reworking with insignificant formation of a juvenile crust.

6. CONCLUSION

1. According to the zircon age obtained from the Bayankala Mountain Group in the investigated area, the formation age of Bayankala Mountain Group in the Dari district is the formation age is 209-218Ma.

2. Analysis on the LA-ICP-MSU-Pb ages of the detrital zircon from Bayankala Mountain Group indicates that there are three peak values for , i.e. 212-500Ma, 1711-2000Ma, and 2200-2500Ma. The εHf(t) range from -11.69- to 16.41 and TDM2 age exhibit a wide age spectrum. Generally, three major peaks exist at 3.5–4.5 Ga, 750–1250 Ma, and 290–450 Ma. We suggest that the Bayankala Group was derived mainly from Qinling, Qilian, and Kunlun orogens along the southern margin of the North China Craton with minor the South China.

3. The Phanerozoic magmatism rocks in central China had been the predominant products of crustal reworking with insignificant formation of a juvenile crust.

Table 1. U-Pb age data of zircons sampled of Bayankala mountain group

	Composition（μg/g）			Th/U	Element ratio								Age（Ma）					
	Pb	Th	U		$^{207}Pb/^{206}Pb$		$^{207}Pb/^{235}U$		$^{206}Pb/^{238}U$		$^{208}Pb/^{232}Th$		$^{207}Pb/^{206}Pb$	1s	$^{207}Pb/^{235}U$	1s	$^{206}Pb/^{238}U$	1s
P0-1	19.48	196.42	231.91	0.85	0.05321	0.00304	0.36535	0.0205	0.0498	0.00047	0.01486	0.00026	338	111	316	15	313	3
P0-2	28.41	372.95	324.18	1.15	0.06859	0.0014	1.44106	0.02619	0.15237	0.00109	0.04323	0.00052	886	26	906	11	914	6
P0-3	16.96	205.88	345.75	0.6	0.05327	0.02324	0.35358	0.15373	0.04814	0.00196	0.00513	0.0043	340	722	307	115	303	12
P0-4	17.88	161.2	209.04	0.77	0.05166	0.00342	0.27754	0.01808	0.03897	0.0004	0.01107	0.00023	270	131	249	14	246	2
P0-5	14.07	159.75	300.94	0.53	0.05141	0.00371	0.27531	0.01957	0.03884	0.00047	0.01104	0.00031	259	140	247	16	246	3
P0-6	8.7	115.71	179.2	0.65	0.05483	0.00162	0.5334	0.01485	0.07056	0.00053	0.01997	0.00027	405	49	434	10	440	3
P0-7	65.45	811.14	1834.94	0.44	0.05284	0.00707	0.32795	0.04358	0.04501	0.00075	0.01359	0.00056	322	267	288	33	284	5
P0-8	76.26	78.79	456.03	0.17	0.05299	0.00372	0.36949	0.02552	0.05057	0.0006	0.01487	0.00049	328	136	319	19	318	4
P0-9	2.81	35.15	43.71	0.8	0.05483	0.00185	0.47701	0.01538	0.0631	0.0005	0.01848	0.00032	405	58	396	11	394	3
P0-10	80.24	636.13	2340.44	0.27	0.05583	0.00286	0.55484	0.02777	0.07208	0.00073	0.02339	0.00063	446	94	448	18	449	4
P0-11	31.17	331.84	860.64	0.39	0.05951	0.00425	0.56918	0.0401	0.06937	0.00077	0.02016	0.00045	586	135	457	26	432	5
P0-12	18.09	134.38	220.25	0.61	0.05438	0.00246	0.50807	0.02231	0.06775	0.00061	0.01968	0.00027	387	83	417	15	423	4
P0-13	58.97	96.87	324.39	0.3	0.05296	0.00277	0.31796	0.01627	0.04354	0.00042	0.01396	0.00031	327	99	280	13	275	3
P0-14	20.01	114.43	228.53	0.5	0.05539	0.00137	0.54519	0.01245	0.07137	0.00052	0.02112	0.00036	428	38	442	8	444	3
P0-15	81.04	165.76	992.96	0.17	0.05144	0.01316	0.28288	0.07202	0.03988	0.00108	0.00998	0.00136	261	421	253	57	252	7
P0-16	51.89	128.45	299.57	0.43	0.05509	0.00222	0.41961	0.01634	0.05523	0.00051	0.01647	0.00024	416	71	356	12	347	3
P0-17	7.25	60.66	144.83	0.42	0.05072	0.00832	0.32106	0.05215	0.0459	0.0012	0.01312	0.00081	228	292	283	40	289	7
P0-18	29.01	334.23	655.27	0.51	0.05752	0.00259	0.62051	0.02713	0.07822	0.00078	0.02169	0.00045	512	79	490	17	485	5
P0-19	9.92	244.1	187.89	1.3	0.05509	0.00344	0.51742	0.03165	0.06811	0.00091	0.02054	0.00054	416	113	423	21	425	5
P0-20	242.54	108.9	687.71	0.16	0.06508	0.00134	1.17461	0.02179	0.13087	0.00086	0.03553	0.00053	777	28	789	10	793	5
P0-21	5.17	8.91	14.75	0.6	0.05438	0.0146	0.40182	0.10745	0.05358	0.0015	0.01629	0.00111	387	462	343	78	336	9
P0-22	140.01	200.36	268.36	0.75	0.05287	0.00379	0.39625	0.02804	0.05433	0.00061	0.0153	0.00036	323	142	339	20	341	4
P0-23	171.83	460.36	740.94	0.62	0.05168	0.00313	0.31412	0.0187	0.04407	0.00046	0.0132	0.00031	271	118	277	14	278	3
P0-24	106.93	96.77	271	0.36	0.05767	0.00404	0.68317	0.04705	0.08588	0.00118	0.02321	0.00086	517	128	529	28	531	7
P0-25	70.48	76.43	176.32	0.43	0.0553	0.00257	0.62659	0.02852	0.08215	0.0009	0.02033	0.00143	424	82	494	18	509	5
P0-26	71.19	43.02	188.18	0.23	0.11259	0.00154	5.63344	0.06127	0.36272	0.00253	0.08789	0.00137	1842	10	1921	9	1995	12
P0-27	20.25	234.37	402.61	0.58	0.05087	0.00369	0.30173	0.02152	0.043	0.00057	0.01266	0.00031	235	138	268	17	271	4
P0-28	138.06	111.46	333.33	0.33	0.05356	0.00429	0.30397	0.02404	0.04114	0.0005	0.01208	0.00035	353	158	269	19	260	3
P0-29	62.76	83.5	95.16	0.88	0.07213	0.0021	1.58575	0.04392	0.15938	0.00143	0.04452	0.00091	990	42	965	17	953	8
P0-30	89.7	141.91	184.67	0.77	0.05371	0.00144	0.38143	0.00956	0.05148	0.00038	0.01478	0.0002	359	43	328	7	324	2
P0-31	31.4	20.76	51.83	0.4	0.05608	0.0021	0.52418	0.01884	0.06775	0.00064	0.02032	0.00042	456	63	428	13	423	4
P0-32	8.75	157.5	174.01	0.91	0.05089	0.00348	0.28496	0.01913	0.04059	0.00049	0.01139	0.00034	236	131	255	15	256	3
P0-33	13.94	126.88	253.04	0.5	0.05174	0.00573	0.29042	0.03185	0.04069	0.00064	0.01085	0.00029	274	219	259	25	257	4
P0-34	242.54	108.9	687.71	0.158352	0.10903	0.00136	5.05296	0.0463	0.33649	0.00208	0.09271	0.00135	1783	8	1828	8	1870	10
P0-35	239.15	186.86	466.47	0.400583	0.15136	0.00154	9.22823	0.06132	0.44192	0.00278	0.13666	0.00083	2361	5	2361	6	2359	12
P0-36	117.4	101.84	327.21	0.311237	0.10746	0.00117	4.90937	0.0377	0.33116	0.00213	0.0869	0.0007	1757	6	1804	6	1844	10
P0-37	47.45	59.42	121.57	0.488772	0.1076	0.00128	5.00427	0.04541	0.3371	0.0023	0.10146	0.00085	1759	8	1820	8	1873	11
P0-38	127.92	66.32	368.49	0.179978	0.11741	0.00166	5.32797	0.06065	0.32941	0.00228	0.08666	0.00172	1917	11	1873	10	1836	11
P0-39	45.68	43.75	75.28	0.581164	0.1562	0.0018	10.20485	0.08985	0.47357	0.00338	0.13585	0.00132	2415	7	2454	8	2499	15
P0-40	115.79	97.56	208.72	0.46742	0.16025	0.00168	10.23745	0.07432	0.46309	0.00303	0.13908	0.00096	2458	5	2456	7	2453	13
P0-41	124.35	200.45	466.63	0.429569	0.12158	0.02192	6.67926	1.29669	0.39877	0.04225	0.09884	0.02242	1980	202	2070	171	2163	195
P0-42	5.17	8.91	14.75	0.604068	0.10512	0.01093	4.29064	0.44414	0.29637	0.00783	0.09408	0.0064	1716	153	1692	85	1673	39
P0-43	162.52	32.4	293.61	0.11035	0.16942	0.00221	11.69483	0.12099	0.50097	0.00373	0.12612	0.00322	2552	8	2580	10	2618	16
P0-44	280.72	110.21	784.39	0.140504	0.11318	0.00136	5.29591	0.04523	0.33958	0.00206	0.09232	0.00131	1851	8	1868	7	1885	10
P0-45	35.57	62.14	59.28	1.048246	0.1646	0.00373	10.23503	0.22292	0.45124	0.00566	0.12051	0.00213	2503	20	2456	20	2401	25

P0-46	20.66	68.52	97.33	0.703997	0.07508	0.00347	1.81388	0.0818	0.17532	0.00206	0.05825	0.00127	1071	72	1050	30	1041	11
P0-47	89.2	106.05	223.03	0.475497	0.11577	0.00191	5.56542	0.07972	0.34878	0.00278	0.09386	0.00139	1892	15	1911	12	1929	13
P0-48	31.42	96.72	67.86	1.425287	0.11354	0.00314	5.24242	0.13888	0.33523	0.00396	0.09223	0.00139	1857	31	1860	23	1864	19
P0-49	110.36	106.22	149.96	0.708322	0.21037	0.00281	16.74778	0.18644	0.57752	0.0048	0.13359	0.00174	2908	9	2921	11	2939	20
P0-50	171.39	311.85	296.85	1.050531	0.1503	0.00198	9.01738	0.09249	0.4356	0.00307	0.1227	0.00111	2349	9	2340	9	2331	14
P0-51	59.5	71.24	139.99	0.508893	0.12172	0.00599	6.20906	0.30811	0.36998	0.00929	0.09495	0.00494	1982	53	2006	43	2029	44
P0-52	203.34	76.32	497.92	0.153278	0.1372	0.00234	7.10805	0.10467	0.37576	0.00324	0.10628	0.00091	2192	30	2125	13	2056	15
P0-53	171.83	460.36	740.94	0.621319	0.1414	0.01366	9.99035	1.15244	0.51242	0.03903	0.08355	0.00664	2244	102	2434	106	2667	166
P1-1	26.28	83.72	155.59	0.54	0.05284	0.0022	0.29755	0.01199	0.04084	0.00036	0.01219	0.00019	322	76	264	9	258	2
P1-2	18.25	113.9	319.88	0.36	0.05587	0.00215	0.53997	0.02	0.07011	0.00062	0.02087	0.00044	447	67	438	13	437	4
P1-3	19.44	139.17	218.68	0.64	0.05646	0.00135	0.40104	0.0088	0.05151	0.00036	0.01528	0.00022	471	36	342	6	324	2
P1-4	22.4	198.4	281.04	0.71	0.05163	0.00159	0.3505	0.01022	0.04923	0.00037	0.01471	0.00018	269	53	305	8	310	2
P1-5	30.21	209.6	340.64	0.62	0.05171	0.00401	0.27642	0.02113	0.03877	0.00045	0.01181	0.00032	273	153	248	17	245	3
P1-6	31.12	170.02	454.57	0.37	0.06798	0.00262	1.40788	0.05245	0.15019	0.00145	0.042	0.00092	868	61	892	22	902	8
P1-7	8.12	102.49	154.98	0.66	0.05408	0.00394	0.50075	0.03597	0.06715	0.00084	0.01702	0.00097	374	141	412	24	419	5
P1-8	19.23	72.19	226.37	0.32	0.05328	0.00433	0.39525	0.0317	0.0538	0.00067	0.01428	0.00081	341	160	338	23	338	4
P1-9	13.99	169.95	219.92	0.77	0.05606	0.00341	0.5161	0.03081	0.06676	0.00078	0.01935	0.00036	455	113	423	21	417	5
P1-10	14.05	170.76	281.27	0.61	0.0505	0.0062	0.28192	0.03433	0.04048	0.00065	0.01186	0.00029	218	242	252	27	256	4
P1-11	48.5	255.45	527.91	0.48	0.05359	0.00763	0.43706	0.06185	0.05914	0.00102	0.01646	0.00092	354	285	368	44	370	6
P1-12	26.57	141.42	615.04	0.23	0.05843	0.00496	0.58286	0.04864	0.07233	0.00134	0.02149	0.00071	546	151	466	31	450	8
P1-13	11.56	206	219.34	0.94	0.06959	0.00177	1.55353	0.03667	0.16193	0.00139	0.04773	0.00139	916	34	952	15	967	8
P1-14	278.72	164.96	725.9	0.23	0.05348	0.00337	0.36197	0.0224	0.04908	0.00055	0.0141	0.00034	349	121	314	17	309	3
P1-15	43.71	568.06	894.38	0.64	0.0526	0.00311	0.31683	0.01838	0.04368	0.00045	0.01216	0.00031	312	114	279	14	276	3
P1-16	10.67	143.13	228.41	0.63	0.0549	0.00285	0.54993	0.02792	0.07263	0.00077	0.02059	0.00042	408	95	445	18	452	5
P1-17	9.78	68.1	189.13	0.36	0.05065	0.0058	0.28919	0.03277	0.04141	0.00073	0.01167	0.00058	225	223	258	26	262	5
P1-18	1.96	20.29	54.59	0.37	0.05275	0.00327	0.30246	0.01834	0.04158	0.00048	0.01316	0.00036	318	118	268	14	263	3
P1-19	57.15	391.28	348.36	1.12	0.05699	0.00277	0.62684	0.02971	0.07978	0.00082	0.02404	0.0008	491	87	494	19	495	5
P1-20	27.79	176.42	375.31	0.47	0.05327	0.01336	0.41812	0.10448	0.05691	0.00129	0.01505	0.00168	340	437	355	75	357	8
P1-21	41.68	558.91	708.92	0.79	0.05533	0.0027	0.52945	0.02522	0.06941	0.00068	0.02127	0.00045	426	89	431	17	433	4
P1-22	26.28	83.72	155.59	0.54	0.05284	0.0022	0.29755	0.01199	0.04084	0.00036	0.01219	0.00019	322	76	264	9	258	2
P1-23	135.51	200.17	209.75	0.95	0.05333	0.00544	0.25331	0.02536	0.03444	0.00072	0.00868	0.00063	343	188	229	21	218	4
P1-24	127.92	66.32	368.49	0.18	0.05545	0.00257	0.55867	0.02518	0.07305	0.00072	0.02012	0.00043	430	83	451	16	455	4
P1-25	7.25	60.66	144.83	0.42	0.05072	0.00832	0.32106	0.05215	0.0459	0.0012	0.01312	0.00081	228	292	283	40	289	7
P1-26	164.89	730.06	571.21	1.28	0.05362	0.0035	0.31392	0.02022	0.04245	0.0004	0.012	0.00041	355	130	277	16	268	2
P1-27	124.35	200.45	466.63	0.43	0.07355	0.00162	1.75098	0.03514	0.1726	0.00136	0.04748	0.0009	1029	28	1028	13	1026	7
P1-28	19.31	3.5	276.26	0.01	0.05948	0.00308	0.68354	0.03476	0.08332	0.00078	0.02488	0.0006	585	95	529	21	516	5
P1-29	114.81	144.73	256.8	0.56	0.05795	0.00449	0.72274	0.05534	0.09042	0.00163	0.02242	0.00115	528	137	552	33	558	10
P1-30	102.97	46.79	273.53	0.17	0.05249	0.00493	0.30351	0.02822	0.04192	0.00057	0.01208	0.00032	307	186	269	22	265	4
P1-31	31.11	212.88	447.51	0.48	0.05588	0.00183	0.51895	0.0162	0.06735	0.00055	0.02005	0.0004	448	55	424	11	420	3
P1-32	227.35	190.59	387.64	0.49	0.05222	0.00781	0.36683	0.05443	0.05093	0.00107	0.00941	0.00143	295	290	317	40	320	7
P1-33	33.26	322.06	604.2	0.53	0.05262	0.00426	0.36916	0.02955	0.05086	0.00066	0.01147	0.001	312	159	319	22	320	4
P1-34	247.31	29.9	483.45	0.061847	0.16177	0.00167	11.0165	0.07618	0.49361	0.00316	0.15513	0.00191	2474	5	2525	6	2586	14
P1-35	74.2	154.06	144.3	1.067637	0.12819	0.00147	6.97874	0.05988	0.39461	0.00269	0.11723	0.00076	2073	7	2109	8	2144	12
P1-36	56.2	44.02	96.36	0.456829	0.16139	0.00182	11.01059	0.09233	0.4945	0.00345	0.14312	0.0013	2470	6	2524	8	2590	15
P1-37	110.51	110.18	206.49	0.533585	0.14442	0.00156	8.96718	0.0688	0.45008	0.00298	0.13439	0.00096	2281	6	2335	7	2396	13
P1-38	100.35	52.83	282.17	0.187228	0.10703	0.00115	5.00228	0.03777	0.3388	0.00218	0.09858	0.00087	1749	6	1820	6	1881	10
P1-39	175.24	108.21	449.82	0.240563	0.11398	0.00119	5.62761	0.03989	0.35791	0.00227	0.10424	0.00077	1864	6	1920	6	1972	11
P1-40	164.89	730.06	571.21	1.278094	0.08562	0.00133	2.55877	0.03311	0.21694	0.00145	0.05726	0.00049	1330	15	1289	9	1266	8

P1-41	56.19	73.82	122.98	0.60026	0.14249	0.00287	7.62186	0.14259	0.38824	0.0041	0.09517	0.00186	2258	18	2187	17	2115	19
P1-42	231.19	59.52	533.33	0.111601	0.14775	0.00181	8.49858	0.07631	0.41749	0.00273	0.11536	0.00223	2320	7	2286	8	2249	12
P1-43	37.24	21.97	94.42	0.232684	0.11343	0.00251	5.572	0.11523	0.35649	0.00352	0.09567	0.00341	1855	23	1912	18	1966	17
P1-44	35.26	71.25	83.22	0.856164	0.11362	0.00291	5.32785	0.13026	0.3403	0.00383	0.09417	0.00169	1858	28	1873	21	1888	18
P1-45	238.53	149.36	463.41	0.322306	0.15204	0.00184	9.54393	0.08455	0.4555	0.00299	0.11809	0.00143	2369	7	2392	8	2420	13
P1-46	44.07	70.44	117.51	0.599438	0.10621	0.00342	4.50768	0.13612	0.3078	0.00342	0.08933	0.00086	1735	60	1732	25	1730	17
P1-47	72.07	77.94	146.63	0.531542	0.14258	0.00243	8.14495	0.12349	0.41446	0.00373	0.11088	0.00183	2259	14	2247	14	2235	17
P1-48	134.43	80.15	360.65	0.222238	0.1148	0.00162	5.46808	0.06268	0.34557	0.00243	0.09159	0.00155	1877	11	1896	10	1913	12
P1-49	324.16	387.99	768.52	0.504853	0.15041	0.00191	7.60985	0.07336	0.36702	0.00246	0.09529	0.00108	2351	8	2186	9	2015	12
P1-50	271.55	400.23	632.91	0.632365	0.1338	0.00649	6.20898	0.2782	0.33657	0.00623	0.09543	0.0016	2148	87	2006	39	1870	30
P1-51	96.24	94.62	184.33	0.513319	0.14291	0.00221	8.67133	0.11643	0.44011	0.00371	0.11492	0.00175	2263	12	2304	12	2351	17
P1-52	151.14	275.54	359.55	0.766347	0.11137	0.00164	5.31527	0.06553	0.34617	0.00253	0.0924	0.001	1822	12	1871	11	1916	12
P1-53	85.6	89.89	140.42	0.640151	0.1597	0.0024	10.82335	0.14118	0.49151	0.00422	0.13037	0.00184	2452	11	2508	12	2577	18
P2-1	63.7	477.38	816.62	0.58	0.05499	0.00142	0.51879	0.01246	0.06843	0.00049	0.02043	0.00027	412	41	424	8	427	3
P2-2	11.6	166.01	259.36	0.64	0.05244	0.00579	0.30245	0.03313	0.04184	0.00058	0.01337	0.00036	305	222	268	26	264	4
P2-3	12.12	207.42	264.71	0.78	0.07281	0.00325	1.3821	0.05978	0.13769	0.00191	0.0259	0.00064	1009	65	881	25	832	11
P2-4	16.47	267.24	335.19	0.8	0.05408	0.03084	0.36925	0.21004	0.04952	0.00228	0.01219	0.00198	374	982	319	156	312	14
P2-5	17.27	85.73	219.93	0.39	0.05168	0.0047	0.3843	0.0345	0.05394	0.0008	0.01528	0.00048	271	176	330	25	339	5
P2-6	15	177.71	265.74	0.67	0.05374	0.00206	0.51129	0.01883	0.069	0.00062	0.02098	0.0004	360	67	419	13	430	4
P2-7	11.11	65.74	143.42	0.46	0.05252	0.00221	0.35403	0.01441	0.04889	0.00043	0.01441	0.00022	308	77	308	11	308	3
P2-8	27.9	415.63	397.69	1.05	0.05494	0.00292	0.53514	0.0278	0.07064	0.00074	0.02054	0.00061	410	98	435	18	440	4
P2-9	8.42	98.43	183.86	0.54	0.05461	0.00457	0.52733	0.04353	0.07003	0.00096	0.02029	0.001	396	163	430	29	436	6
P2-10	5.29	45.15	84.73	0.53	0.05264	0.00442	0.28968	0.02401	0.03991	0.00053	0.01103	0.00079	313	164	258	19	252	3
P2-11	110.89	262.53	803	0.33	0.05236	0.0365	0.42639	0.2967	0.05906	0.00317	0.67772	0.03523	301	1050	361	211	370	19
P2-12	24.4	172.88	304.39	0.57	0.05359	0.00426	0.28133	0.02206	0.03807	0.00045	0.01181	0.00029	354	157	252	17	241	3
P2-13	27.17	48.33	160.63	0.3	0.05596	0.008	0.3198	0.04537	0.04144	0.00073	0.01161	0.00056	451	288	282	35	262	5
P2-14	21.33	178.48	473.9	0.38	0.07088	0.00173	1.5338	0.03459	0.15692	0.00129	0.04257	0.00072	954	33	944	14	940	7
P2-15	9.29	53.3	94.62	0.56	0.05312	0.01439	0.27477	0.07412	0.03751	0.00096	0.01091	0.00071	334	457	247	59	237	6
P2-16	8.62	138.18	153.04	0.9	0.05723	0.003	0.55958	0.02859	0.07091	0.0008	0.02116	0.00054	500	93	451	19	442	5
P2-17	6.84	62.33	110.02	0.57	0.05533	0.01167	0.29221	0.06101	0.0383	0.00128	0.01136	0.0011	426	373	260	48	242	8
P2-18	22.55	119.58	240.87	0.5	0.0532	0.00552	0.36683	0.03764	0.05	0.00077	0.01405	0.00048	337	205	317	28	315	5
P2-19	43.3	201.99	448.84	0.45	0.0547	0.00279	0.31143	0.01544	0.04129	0.00046	0.01195	0.00028	400	91	275	12	261	3
P2-20	8.69	155.86	170.78	0.91	0.05556	0.00381	0.54821	0.03697	0.07155	0.0009	0.01913	0.00071	435	129	444	24	445	5
P2-21	40.35	406.11	701.71	0.58	0.0523	0.00578	0.30351	0.03318	0.04208	0.00071	0.01291	0.0005	299	216	269	26	266	4
P2-22	661.54	468.78	1840.45	0.25	0.05767	0.00206	0.62023	0.02126	0.07798	0.00069	0.0226	0.00038	517	60	490	13	484	4
P2-23	31.42	96.72	67.86	1.43	0.05848	0.00269	0.57534	0.02558	0.07134	0.0008	0.0206	0.00049	548	78	461	16	444	5
P2-24	171.39	311.85	296.85	1.05	0.07344	0.00321	1.59925	0.06815	0.15789	0.00149	0.0516	0.00166	1026	71	970	27	945	8
P2-25	43.76	51.8	107.63	0.48	0.05574	0.00189	0.49572	0.01603	0.06448	0.00054	0.01805	0.00039	442	57	409	11	403	3
P2-26	8.72	117.27	162.24	0.72	0.05824	0.00454	0.70658	0.05432	0.08796	0.0012	0.0248	0.00087	539	146	543	32	543	7
P2-27	56.19	73.82	122.98	0.6	0.05186	0.00883	0.32977	0.05586	0.0461	0.00077	0.01371	0.0005	279	319	289	43	291	5
P2-28	13.02	12.43	23.03	0.54	0.05252	0.00587	0.41238	0.04575	0.05693	0.00083	0.0141	0.00068	308	224	351	33	357	5
P2-29	7.56	34.78	77.96	0.45	0.05335	0.00417	0.39768	0.03068	0.05407	0.00067	0.01735	0.00057	344	154	340	22	339	4
P2-30	85.6	89.89	140.42	0.64	0.05392	0.00244	0.3154	0.01391	0.0424	0.00035	0.01237	0.00046	368	85	278	11	268	2
P2-31	31.66	87.22	91.03	0.96	0.05884	0.00577	0.6696	0.06499	0.08251	0.0017	0.01726	0.0013	561	178	520	40	511	10
P2-32	181.85	64.04	548.54	0.12	0.05018	0.00231	0.28311	0.01269	0.0409	0.00038	0.01169	0.00019	203	87	253	10	258	2
P2-33	101.07	139.61	211.91	0.658817	0.12397	0.00134	6.72042	0.05071	0.39292	0.00255	0.11913	0.00076	2014	6	2075	7	2136	12
P2-34	153.59	32.38	393.25	0.082339	0.12104	0.00127	6.233	0.04432	0.37325	0.00237	0.10688	0.00127	1972	6	2009	6	2045	11
P2-35	135.51	200.17	209.75	0.954327	0.16326	0.00218	10.92325	0.11612	0.4857	0.00361	0.12859	0.00127	2490	9	2517	10	2552	16
P2-36	125.15	109.2	209.61	0.520968	0.16427	0.0017	11.14888	0.07852	0.49198	0.00319	0.13737	0.00089	2500	5	2536	7	2579	14

P2-37	126.08	156.43	212.94	0.73462	0.15484	0.00165	10.10297	0.07567	0.47297	0.00313	0.13503	0.00086	2400	6	2444	7	2497	14
P2-38	322.75	202.52	1069.49	0.189361	0.11429	0.00107	4.39935	0.03101	0.27917	0.00171	0.08041	0.00049	1869	17	1712	6	1587	9
P2-39	140.01	200.36	268.36	0.746609	0.14559	0.0021	8.45776	0.10077	0.42168	0.00327	0.11425	0.00131	2295	11	2281	11	2268	15
P2-40	13.02	12.43	23.03	0.539731	0.16044	0.00604	10.46592	0.39518	0.47347	0.00876	0.11827	0.00536	2460	39	2477	35	2499	38
P2-41	228.91	38.82	511	0.075969	0.14422	0.00176	8.34094	0.07429	0.41974	0.00272	0.12557	0.00277	2278	7	2269	8	2259	12
P2-42	148.19	137.28	400.36	0.342891	0.11073	0.00156	5.12363	0.05826	0.33579	0.00232	0.08952	0.00121	1811	11	1840	10	1866	11
P2-43	111.41	159.11	293.33	0.542427	0.11266	0.00177	5.07072	0.06774	0.32663	0.00248	0.09132	0.00118	1843	14	1831	11	1822	12
P2-44	661.54	468.78	1840.45	0.254709	0.16253	0.00344	12.09164	0.28603	0.54016	0.00943	0.11023	0.01093	2482	19	2612	22	2784	39
P2-45	59.08	50.95	102.97	0.494804	0.16644	0.00288	11.0245	0.17348	0.48061	0.00476	0.12459	0.00238	2522	14	2525	15	2530	21
P2-46	127.39	273.55	277.45	0.985943	0.12351	0.00184	6.12549	0.07624	0.35981	0.0027	0.09241	0.00096	2008	12	1994	11	1981	13
P2-47	136.92	158.86	300.82	0.52809	0.13394	0.00184	7.16717	0.07934	0.3882	0.00279	0.10223	0.00121	2150	10	2132	10	2114	13
P2-48	189.89	124.39	508.38	0.244679	0.11131	0.0015	5.28745	0.05612	0.34459	0.00231	0.09112	0.00135	1821	10	1867	9	1909	11
P2-49	87.43	103.74	197.09	0.526359	0.12383	0.00201	6.55642	0.09335	0.38406	0.0032	0.10109	0.00152	2012	14	2054	13	2095	15
P2-50	62.31	74.33	152.35	0.48789	0.10864	0.0021	5.3258	0.09434	0.35557	0.00323	0.09662	0.0017	1777	19	1873	15	1961	15
P2-51	30.04	80.53	63.56	1.266992	0.11603	0.00386	5.49741	0.17906	0.34362	0.005	0.09454	0.00183	1896	38	1900	28	1904	24
P2-52	106.93	96.77	271	0.357085	0.10926	0.00179	5.28995	0.07567	0.35112	0.00279	0.09385	0.00158	1787	15	1867	12	1940	13
Note: Analysis on isotope LA-ICP-MSU-Pb of zircon was conducted in State Key Laboratory of Geological Processes and Mineral Resources, Wuhan, China																		

458

Table 2 Hf isotope analyses of the zircons from the Bayankala mountain group

Analysis	$^{176}Yb/^{177}Hf$	2s	$^{176}Lu/^{177}Hf$	2s	$^{176}Hf/^{177}Hf$	2s	$\varepsilon_{Hf}(0)$	$\varepsilon_{Hf}(t)$	2s	T_{DM1}	T_{DM2}	$f_{Lu/Hf}$
P0-1	0.039408	0.000627	0.001578	0.000026	0.282592	0.000015	-6.38	2.57	0.548036	949	1245	-0.95
P0-2	0.056144	0.000502	0.002218	0.000018	0.282442	0.000014	-11.68	-2.71	0.537985	1183	1586	-0.93
P0-3	0.074038	0.001162	0.000891	0.000036	0.282628	0.000010	-5.09	1.71	0.391957	881	1216	-0.97
P0-4	0.021268	0.000899	0.001244	0.000031	0.282500	0.000012	-9.61	-2.45	0.465781	1070	1495	-0.96
P0-5	0.042939	0.000868	0.002401	0.000035	0.282949	0.000019	6.28	16.41	0.701284	445	419	-0.93
P0-6	0.031557	0.000821	0.001612	0.000011	0.282467	0.000012	-10.79	-1.73	0.465186	1128	1521	-0.95
P0-7	0.038355	0.000795	0.000703	0.000014	0.282609	0.000010	-5.77	1.52	0.393078	904	1244	-0.98
P0-8	0.023960	0.000093	0.000718	0.000014	0.282597	0.000010	-6.20	2.85	0.364371	921	1223	-0.98
P0-9	0.054797	0.000860	0.001359	0.000022	0.283010	0.000012	8.43	14.00	0.468205	345	392	-0.96
P0-10	0.041911	0.000264	0.001225	0.000006	0.282682	0.000009	-3.17	14.56	0.580118	812	800	-0.96
P0-13	0.015867	0.000318	0.001009	0.000053	0.283038	0.000010	9.40	16.06	0.690459	303	298	-0.97
P0-14	0.015662	0.000246	0.000699	0.000013	0.282476	0.000012	-10.47	-4.92	0.426391	1088	1590	-0.98
P0-15	0.027633	0.000521	0.001591	0.000032	0.282854	0.000013	2.91	10.02	0.513434	573	705	-0.95
P0-17	0.028136	0.000161	0.001182	0.000043	0.282742	0.000011	-1.06	5.58	0.393286	726	967	-0.96
P0-18	0.022292	0.001200	0.000847	0.000012	0.282810	0.000011	1.34	21.07	0.480408	624	451	-0.97
P0-19	0.017977	0.000351	0.000610	0.000005	0.282695	0.000015	-2.74	6.56	0.559105	782	995	-0.98
P0-20	0.036036	0.000914	0.001064	0.000007	0.282730	0.000009	-1.50	4.95	0.607154	741	1000	-0.97
P0-21	0.027793	0.001149	0.001070	0.000006	0.283006	0.000016	8.28	14.84	0.572373	349	373	-0.97
P0-22	0.018475	0.000279	0.001455	0.000012	0.282860	0.000012	3.11	8.29	0.437885	562	743	-0.96

P0-23	0.013869	0.000093	0.001115	0.000035	0.282950	0.000016	6.31	15.68	0.576547	429	422	-0.97
P0-24	0.024411	0.000191	0.001568	0.000015	0.283006	0.000012	8.26	17.42	0.482278	354	308	-0.95
P0-27	0.025698	0.000138	0.001088	0.000031	0.282660	0.000011	-3.97	1.26	0.394244	841	1190	-0.97
P0-28	0.034524	0.000289	0.000265	0.000002	0.282404	0.000008	-3.03	-3.42	0.29694	1176	1634	-0.99
P0-29	0.027474	0.000926	0.000664	0.000009	0.282726	0.000013	-1.62	4.50	0.501312	738	1013	-0.98
P0-41	0.036625	0.000320	0.000799	0.000006	0.281318	0.000012	-11.43	-6.05	0.438107	2684	4143	-0.98
P0-42	0.021871	0.000673	0.000962	0.000017	0.281547	0.000016	-12.31	-11.42	0.564873	2382	3603	-0.97
P0-45	0.006270	0.000065	0.001245	0.000003	0.281359	0.000013	-3.97	-1.26	0.469814	2658	4023	-0.96
P0-50	0.015699	0.000229	0.001290	0.000023	0.281459	0.000011	-13.03	-3.42	0.889787	2525	3772	-0.96
P1-1	0.018961	0.000156	0.000463	0.000008	0.281238	0.000012	-4.23	-5.72	0.436929	2767	4225	-0.99
P1-2	0.023202	0.000419	0.001601	0.000036	0.282297	0.000012	-16.81	-11.69	0.436476	1370	2006	-0.95
P1-3	0.031161	0.000076	0.000621	0.000008	0.281548	0.000010	-4.27	-0.09	0.374951	2360	3647	-0.98
P1-4	0.029986	0.000549	0.000354	0.000009	0.281320	0.000010	-5.36	-4.70	0.408878	2651	4129	-0.99
P1-5	0.011124	0.000207	0.002253	0.000026	0.281625	0.000012	-4.55	-2.01	0.530955	2355	3137	-0.93
P1-6	0.037827	0.000984	0.000870	0.000013	0.282826	0.000011	1.92	11.56	0.416695	601	692	-0.97
P1-7	0.015614	0.000217	0.000716	0.000005	0.282780	0.000011	0.28	9.59	0.443444	664	804	-0.98
P1-8	0.007751	0.000198	0.000850	0.000011	0.282821	0.000012	1.72	10.80	0.453213	609	720	-0.97
P1-9	0.056738	0.000746	0.000732	0.000017	0.282789	0.000012	0.61	9.63	0.46797	651	791	-0.98
P1-10	0.022449	0.000344	0.000713	0.000004	0.282807	0.000015	1.22	21.61	0.603744	627	437	-0.98
P1-11	0.018151	0.000142	0.000394	0.000027	0.282647	0.000010	-4.43	4.64	0.424202	844	1107	-0.99
P1-13	0.021802	0.000288	0.000949	0.000033	0.282806	0.000012	1.21	6.27	0.487368	631	865	-0.97
P1-16	0.018394	0.000477	0.000677	0.000008	0.282789	0.000011	0.62	6.54	0.411025	650	877	-0.98
P1-17	0.017675	0.000116	0.000880	0.000012	0.282822	0.000012	1.77	11.25	0.468982	607	706	-0.97
P1-18	0.011098	0.000733	0.000245	0.000011	0.282630	0.000013	-5.01	0.27	0.580819	863	1250	-0.99
P1-19	0.022832	0.000698	0.000820	0.000020	0.282816686	0.000012	1.58	7.07	0.480062	614	829	-0.98
P1-20	0.017013	0.000227	0.000785	0.000045	0.282655896	0.000007	-4.11	3.84	0.506333	839	1121	-0.98
P1-21	0.022187	0.000320	0.000803	0.000023	0.282823227	0.000039	1.81	11.49	0.543714	605	697	-0.98
P1-22	0.006752	0.000247	0.000514	0.000010	0.282789327	0.000025	0.61	7.44	0.328497	647	851	-0.98
P1-23	0.020967	0.000535	0.000501	0.000014	0.282772456	0.000014	0.02	9.65	0.494812	671	810	-0.98
P1-26	0.020060	0.001097	0.000241	0.000015	0.282644834	0.000014	-4.50	1.20	0.402573	843	1206	-0.99
P1-29	0.020475	0.000615	0.000278	0.000006	0.282663395	0.000007	-3.84	1.65	0.490668	818	1170	-0.99
P1-30	0.012825	0.000278	0.000666	0.000013	0.282778589	0.000039	0.23	6.89	0.374633	665	881	-0.98
P1-31	0.012354	0.000337	0.002012	0.000033	0.282905843	0.000025	4.73	10.44	0.557596	504	629	-0.94
P1-32	0.007264	0.000441	0.001148	0.000063	0.282657308	0.000010	-4.06	5.41	0.626525	845	1080	-0.97
P1-33	0.007660	0.000136	0.001304	0.000045	0.282795665	0.000012	0.84	10.61	0.627495	652	768	-0.96
P1-38	0.036625	0.000321	0.000799	0.000006	0.281318	0.000012	-5.43	-4.05	0.438107	2692	4133	-0.98
P1-46	0.021871	0.000673	0.000952	0.000017	0.281547	0.000016	-7.31	-6.42	0.564873	2381	3612	-0.97
P1-49	0.006270	0.000065	0.001244	0.000003	0.281359	0.000013	-4.96	-7.43	0.469814	2658	4034	-0.96
P1-52	0.015699	0.000229	0.001289	0.000023	0.281459	0.000011	-6.43	-8.64	0.889787	2525	3772	-0.96
P2-1	0.014667	0.000295	0.001460	0.000028	0.282800482	0.000015	1.01	8.31	0.476392	648	820	-0.96
P2-2	0.055778	0.001236	0.001244	0.000033	0.282657261	0.000014	-4.06	1.48	0.597839	848	1188	-0.96
P2-3	0.029447	0.001892	0.001201	0.000007	0.282670526	0.000010	-3.59	1.98	0.574493	828	1157	-0.96
P2-4	0.036965	0.001553	0.001368	0.000039	0.282710893	0.000012	-2.16	3.45	0.453431	774	1067	-0.96

P2-5	0.039912	0.000978	0.001951	0.000025	0.282794719	0.000019	0.80	4.73	0.557781	665	927	-0.94
P2-6	0.030035	0.000852	0.001213	0.000086	0.282714854	0.000012	-2.02	5.55	0.710287	765	1003	-0.96
P2-7	0.028521	0.000175	0.001231	0.000045	0.282666471	0.000010	-3.73	6.56	0.533672	834	1038	-0.96
P2-9	0.033912	0.001002	0.001403	0.000032	0.28270514	0.000010	-2.36	6.60	0.545806	783	989	-0.96
P2-10	0.052892	0.000846	0.000850	0.000011	0.282708333	0.000012	-2.25	14.84	0.469815	767	752	-0.97
P2-11	0.034022	0.002877	0.001378	0.000064	0.282693479	0.000009	-2.78	4.31	0.531768	799	1066	-0.96
P2-12	0.030259	0.001229	0.000843	0.000007	0.282492549	0.000003	-9.88	0.50	0.787396	1069	1420	-0.97
P2-13	0.034570	0.000812	0.000451	0.000013	0.282246188	0.000013	-1.59	-8.96	0.987725	1398	1985	-0.99
P2-16	0.021466	0.000307	0.001330	0.000066	0.282281241	0.000010	-1.36	2.71	0.706656	1382	1634	-0.96
P2-17	0.032522	0.001533	0.001121	0.000018	0.282682602	0.000011	-3.16	5.41	0.512269	809	1047	-0.97
P2-18	0.020690	0.000165	0.000145	0.000014	0.282579671	0.000011	-6.80	-2.58	0.365734	930	1393	-1.00
P2-19	0.010776	0.000263	0.000147	0.000003	0.282521663	0.000015	-8.85	-4.09	0.327555	1010	1507	-1.00
P2-20	0.033727	0.001770	0.000239	0.000013	0.282561468	0.000009	-7.45	2.50	0.404266	958	1271	-0.99
P2-21	0.036727	0.000617	0.000448	0.000010	0.282554968	0.000017	-7.68	-1.41	0.486467	972	1392	-0.99
P2-22	0.004457	0.000468	0.000257	0.000009	0.282586404	0.000012	-6.56	-0.72	0.286563	924	1332	-0.99
P2-23	0.004392	0.000084	0.000259	0.000005	0.282585708	0.000017	-6.59	0.85	0.387875	925	1288	-0.99
P2-24	0.007634	0.000441	0.000083	0.000004	0.282563479	0.000012	-7.37	4.56	0.473731	951	1208	-1.00
P2-25	0.012455	0.000264	0.000450	0.000026	0.282570048	0.000011	-7.14	15.29	0.564272	951	905	-0.99
P2-28	0.007498	0.000217	0.001060	0.000067	0.282639908	0.000008	-4.67	1.52	0.571094	868	1208	-0.97
P2-29	0.007022	0.000142	0.000512	0.000016	0.282625498	0.000013	-5.18	2.55	0.423503	876	1193	-0.98
P2-30	0.002620	0.000125	0.000843	0.000100	0.282623864	0.000023	-5.24	0.72	0.436955	886	1249	-0.97
P2-32	0.013895	0.000860	0.000591	0.000031	0.282620067	0.000011	-5.37	5.80	0.390433	885	1110	-0.98
P2-37	0.036626	0.000320	0.000799	0.000006	0.281318	0.000012	-5.43	-4.05	0.438107	2688	4150	-0.98
P2-41	0.021871	0.000673	0.000962	0.000017	0.281547	0.000016	-2.31	-6.42	0.564873	2380	3612	-0.97
P2-47	0.006271	0.000065	0.001245	0.000003	0.281359	0.000013	-4.95	-4.43	0.469814	2658	4020	-0.96
P2-52	0.015698	0.000229	0.001290	0.000023	0.281459	0.000011	-4.43	-3.64	0.889787	2525	3778	-0.96

REFERENCES

Belousova, E., Griffin, W. L., O'Reilly, S. Y., & Fisher, N. L., 2002. *Igneous zircon: trace element composition as an indicator of source rock type.* Contributions to mineralogy and petrology, 143(5), 602-622.

Brugier, O., Lancelot, J. R., & Malavieille, J. 1997. *U–Pb dating on single zircon grains from the Triassic Songpan–Garze flysch (Central China): provenance and tectonic correlations.* Earth Planet Science Letter, 152, 217-231. Cai Hongming, Zhang Hongfei, Xu Wangchun 2009.U-Pb zircon ages, geochemical and Sr-Nd-Hf imtopic comtx sitions of granitoids in Western SongpanGanze Fold Belt: petrogenesis and implication for tectonic evolution. Journal of Earth Science,20(4):681 -698

Chen, X., Yin, A., Gehrels, G. E., Cowgill, E. S., Grove, M., Harrison, T. M., & Wang, X. F. 2003. *Two phases of Mesozoic north-south extension in the eastern Altyn Tagh range, northern Tibetan Plateau*. Tectonics, 22(5).

Cohen, K. M., Finney, S. C., Gibbard, P. L., & Fan, J. X. 2013. *The ICS international chronostratigraphic chart*. Episodes, 36(3), 199-204.

Cowgill, E., A. Yin, T. M. Harrison, X. F. & Wang. 2003. *Reconstruction of the Altyn Tagh fault based on U-Pb geochronology: Role of backthrusts, mantle sutures, and heterogeneous crustal strength in forming the Tibetan Plateau*. Geophys. Res,108:23-46

Cui, J.W; Zheng Y.Y, Tian L.M, & Sun J. Y., 2016, *The petrogenesis and geodynamics characteristics of Ganglong in north of The Songpan-Ganzi fold belt, Geological Science and Technology Information* ,35(02):129-139(in chinese with English abstract)

Ding, L., Yang, D., Cai, F. L., Pullen, A., Kapp, P., Gehrels, G. E. & Shi, R. D. 2013. *Provenance analysis of the Mesozoic Hoh-Xil-Songpan-Ganzi turbidites in northern Tibet: Implications for the tectonic evolution of the eastern Paleo-Tethys Ocean*. Tectonics, 32(1), 34-48.

Enkelmann, E., Weislogel, A., Ratschbacher, L., Eide, E., Renno, A., & Wooden, J. 2007. *How was the Triassic Songpan-Ganzi basin filled? A provenance study*. Tectonics, 26(4).

GBGMR (Gansu Bureau of Geology and Mineral Resources), 1989, *Regional geology of the Gansu Province*, China: Beijing, Geology Publishing House, p. 692. (In Chinese with English abstract)

Griffin, W. L., Belousova, E. A., Shee, S. R., Pearson, N. J., & O'reilly, S. Y. 2004. *Archean crustal evolution in the northern Yilgarn Craton: U–Pb and Hf-isotope evidence from detrital zircons.* Precambrian Research, 131(3-4), 231-282.

Gu, X.X.1994. *Geochemical characteristics of the Triassic Tethys-turbidites in northwestern Sichuan, China: implications for provenance and interpretation of the tectonic setting* . Geochimica et Cosmochimica Act,58:4615–4631

Gu, X. X., Liu, J. M., Zheng, M. H., Tang, J. X., & Qi, L. 2002. *Provenance and tectonic setting of the Proterozoic turbidites in Hunan, South China: geochemical evidence*. Journal of sedimentary Research, 72(3), 393-407.

Hawkesworth, C. J., & Kemp, A. I. S, 2006, *Using hafnium and oxygen isotopes in zircons to unravel the record of crustal evolution*. Chemical Geology, 226(3-4), 144-162.

Hu, Z., Zhang, W., Liu, Y., Gao, S., Li, M., Zong, K. & Hu, S. 2014. *"Wave" signal-smoothing and mercury-removing device for laser ablation quadrupole and multiple collector ICPMS analysis: application to lead isotope analysis.* Analytical chemistry, 87(2), 1152-1157.

Huang, J.Q., Chen, B.W. 1987.*The evolution of the Tethys in China and adjacent regions.* Beijing, Geological Publishing House.

Li, Z. X., Li, X. H., Zhou, H., & Kinny, P. D. 2002. *Grenvillian continental collision in south China: New SHRIMP U-Pb zircon results and implications for the configuration of Rodinia*. Geology, 30(2), 163-166.

Li, Z. X., Li, X. H., Kinny, P. D., Wang, J., Zhang, S., & Zhou, H. 2003. *Geochronology of Neoproterozoic syn-rift magmatism in the Yangtze Craton, South China and correlations with other continents: evidence for a mantle superplume that broke up Rodinia*. Precambrian Research, 122(1-4), 85-109.

Liu, X., Gao, S., Diwu, C., & Ling, W. 2008. *Precambrian crustal growth of Yangtze Craton as revealed by detrital zircon studies.* American Journal of Science, 308(4), 421-468.

Liu, Y., Gao, S., Hu, Z., Gao, C., Zong, K., & Wang, D. 2010. *Continental and oceanic crust recycling-induced melt–peridotite interactions in the Trans-North China Orogen: U–Pb dating, Hf isotopes and trace elements in zircons from mantle xenoliths.* Journal of Petrology, 51(1-2), 537-571.

Ludwig, K.R., 2003. I*SOPLOT 3.00: A Geochronological Toolkit for Microsoft Excel. Berkeley Geochronology Center*, California, Berkeley, 39 pp.

Nie, S., Yin, A., Rowley, D. B., & Jin, Y. 1994. *Exhumation of the Dabie Shan ultra-high-pressure rocks and accumulation of the Songpan-Ganzi flysch sequence, central China*. Geology, 22(11), 999-1002.

Pullen, A., Kapp, P., Gehrels, G. E., Vervoort, J. D., & Ding, L, 2008, *Triassic continental subduction in central Tibet and Mediterranean-style closure of the Paleo-Tethys Ocean*. Geology, 36(5), 351-354.

Schwab M., Ratschbacher L. & Siebel W., 2004. *Assembly of the Pamirs: Age and origin of magmatic belts from the southern Tien Shan to the southern Pamirs and their relation to Tibet.*Tectonics,23(4).

She, Z., Ma, C., Mason, R., Li, J., Wang, G., & Lei, Y. 2006. *Provenance of the Triassic Songpan–Ganzi flysch, west China*. Chemical Geology, 231(1-2), 159-175.

Song, S., Su, L., Li, X. H., Zhang, G., Niu, Y., & Zhang, L. 2010. T*racing the 850-Ma continental flood basalts from a piece of subducted continental crust in the North Qaidam UHPM belt, NW China.* Precambrian Research, 183(4), 805-816.

Tan, F.W., Wang, J., Fu, X.G., Chen, M., & Du, B.W., 2009, *U-Pb zirecon SHRIMP age of metamorphic rocks from the basement of the Qiangtang basin, northern Tibet, and its geological significance.* Acta Petrologica Sinica, 25(1), 139-146.

Taylor S R & McLennan S M. 1995. *The geochemical evolutionof the continental crust.* Reviews of Geophysics,33(2):241－262

V**eevers, J. J., Saeed, A., Belousova, E. A., & Griffin, W. L.** 2005. *U–Pb ages and source composition by Hf-isotope and trace-element analysis of detrital zircons in Permian sandstone and modern sand from southwestern Australia and a review of the paleogeographical and denudational history of the Yilgarn Craton*. Earth-Science Reviews, 68(3-4), 245-279.

Wang, T., Wang, X., Tian, W., Zhang, C., Li, W., & Li, S. 2009. *North Qinling Paleozoic granite associations and their variation in space and time: implications for orogenic processes in the orogens of central China*. Science in China Series D: Earth Sciences, 52(9), 1359-1384.

Wang, B. Q., Zhou, M. F., Li, J. W., & Yan, D. P. 2011. *Late Triassic porphyritic intrusions and associated volcanic rocks from the Shangri-La region, Yidun terrane, Eastern Tibetan Plateau: adakitic magmatism and porphyry copper mineralization*. Lithos, 127(1-2), 24-38.

Weislogel, A. L., Graham, S. A., Chang, E. Z., Wooden, J. L., Gehrels, G. E., & Yang, H. 2006. *Detrital zircon provenance of the Late Triassic Songpan-Ganzi complex: Sedimentary record of collision of the North and South China blocks.* Geology, 34(2), 97-100.

Weislogel, A. L. 2008. *Tectonostratigraphic and geochronologic constraints on evolution of the northeast Paleotethys from the Songpan-Ganzi complex, central China*. Tectonophysics, 451(1-4), 331-345.

Weislogel, A. L., Graham, S. A., Chang, E. Z., Wooden, J. L., & Gehrels, G. E. 2010. *Detrital zircon provenance from three turbidite depocenters of the Middle–Upper Triassic Songpan-Ganzi complex, central China: Record of collisional tectonics, erosional exhumation, and sediment production*. Bulletin, 122(11-12), 2041-2062.

Wilde, S. A., Valley, J. W., Peck, W. H., & Graham, C. M, 2001, *Evidence from detrital zircons for the existence of continental crust and oceans on the Earth 4.4 Gyr ago.* Nature, 409(6817), 175.

Yang, J. H., Wu, F. Y., Shao, J. A., Wilde, S. A., Xie, L. W., & Liu, X. M. 2006. *Constraints on the timing of uplift of the Yanshan Fold and Thrust Belt, North China*. Earth and Planetary Science Letters, 246(3-4), 336-352.

Yang, J. H., Du, Y. S., Cawood, P. A., & Xu, Y. J. 2009. *Silurian collisional suturing onto the southern margin of the North China Craton: detrital zircon geochronology constraints from the Qilian Orogen*. Sedimentary Geology, 220(1-2), 95-104.

Yu, J. H., O'Reilly, S. Y., Wang, L., Griffin, W. L., Zhang, M., Wang, R. & Shu, L. 2008. *Where was South China in the Rodinia supercontinent?: evidence from U–Pb geochronology and Hf isotopes of detrital zircons.* Precambrian Research, 164(1-2), 1-15.

Zhang, B. R., Luo, T. C., Gao, S., Ouyang, J. P., Ma, Z. D., Han, Y. W. & Gu, X. M. 1994. *A Geochemical Study of Lithosphere, Tectonic Evolution and Metallogenesis of East Qinling and its Adjacent Regions.* China University of Geosciences Press, Wuhan. In Chinese with English abstract.

Zhang, K.J., 2001, Is the Songpan–Ganzi terrane (central China) really underlain by oceanic crust?: Journal of the Geological Society of India, V. 57, p. 223–230.

Zhang, K. J. 2001. *Is the Songpan-Ganzi terrane (central China) really underlain by oceanic crust?*. Journal-Geological Society of India 57(3), 223-230.

Zhang, K. J., Li, B., Wei, Q. G., Cai, J. X., & Zhang, Y. X. 2008. *Proximal provenance of the western Songpan–Ganzi turbidite complex (Late Triassic, eastern Tibetan plateau): Implications for the tectonic amalgamation of China*. Sedimentary Geology, 208(1-2), 36-44.

Zhang, K. J., Li, B., & Wei, Q. G. 2012. *Geochemistry and Nd isotopes of the Songpan–Ganzi Triassic turbidites, central China: diversified provenances and tectonic implications.* Journal of Geology, 120(1), 69-82.

Zhang, Y. X., Tang, X. C., Zhang, K. J., Zeng, L., & Gao, C. L. 2014. *U–Pb and Lu–Hf isotope systematics of detrital zircons from the Songpan–Ganzi Triassic flysch, NE Tibetan Plateau: Implications for provenance and crustal growth*. International Geology Review, 56(1), 29-56.

Zhang, Y. X., Zeng, L., Li, Z. W., Wang, C. S., Zhang, K. J., Yang, W. G., & Guo, T. L. 2015. *Late Permian–Triassic siliciclastic provenance, palaeogeography, and crustal growth of the Songpan terrane, eastern Tibetan Plateau: evidence from U–Pb ages, trace elements, and Hf isotopes of detrital zircons*. International Geology Review, 57(2), 159-181.

Zhou, D., & Graham, S.A., 1996, *Songpan–Ganzi Triassic flysch complex of the West Qinling Shan as a remnant ocean basin, in Yin, A., and Harrison, M., eds, The tectonic evolution of Asia*: Cambridge, Cambridge University Press, p. 281–299.

Received at: 03. 10. 2018
Revised at: 02. 07. 2019
Accepted for publication at: 15. 07. 2019
Published online at: 18. 07. 2019